AD-A114 772 AERONAUTICAL RESEARCH LABS MELBOURNE (AUSTRALIA) F/G 20/4
A ROTOR WAKE MODEL FOR FORWARD FLIGHT SIMULATION STUDIES,(U)
JUN 81 K R REDDY
UNCLASSIFIED ARL/AERO-NOTE-402 NL

END
DATE
FILMED
6 82
DTIC

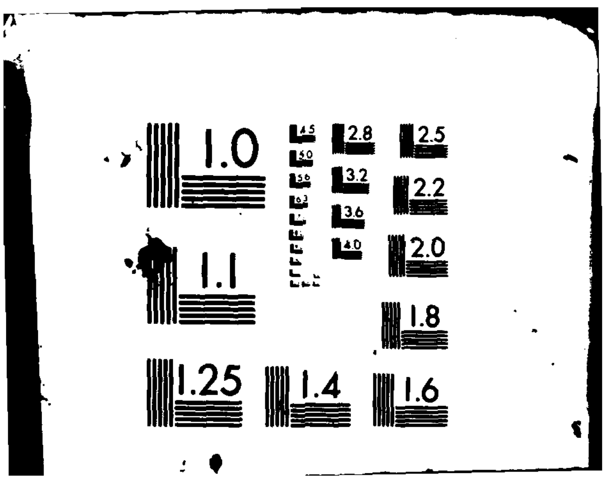
1.0
2.8
2.5
3.2
2.2
3.6
4.0
2.0
1.1
1.8
1.25
1.4
1.6

(12)

ARL-AERO-NOTE-402

AR-002-290

AD A114772

DEPARTMENT OF DEFENCE

DEFENCE SCIENCE AND TECHNOLOGY ORGANISATION

AERONAUTICAL RESEARCH LABORATORIES

MELBOURNE, VICTORIA

AERODYNAMICS NOTE 402

A ROTOR WAKE MODEL FOR FORWARD FLIGHT SIMULATION STUDIES

by

K. R. REDDY

Approved for Public Release.

COPY No

JUNE 1981

AR-002-290

DEPARTMENT OF DEFENCE
DEFENCE SCIENCE AND TECHNOLOGY ORGANISATION
AERONAUTICAL RESEARCH LABORATORIES

AERODYNAMICS NOTE 402

A ROTOR WAKE MODEL FOR FORWARD FLIGHT SIMULATION STUDIES

by

K. R. REDDY

SUMMARY

This Note presents an attempt to develop a rotor wake model for forward flight which requires only modest computing time and, therefore, is suitable for simulation studies. Free and rigid wake models are discussed, together with various simplifying assumptions, in order to reduce the computation time to acceptable levels for simulation studies. Using a tip vortex wake model and the Biot–Savart relation, induced velocities are calculated in the rotor plane. It is then assumed that the tip vortex wake takes the form of a skewed helix. Such a simple prescribed model requires little computing time and the accuracy of its results when compared with more elaborate free wake models shows considerable promise.

POSTAL ADDRESS: Chief Superintendent, Aeronautical Research Laboratories,
Box 4331, P.O., Melbourne, Victoria, 3001, Australia.

DOCUMENT CONTROL DATA SHEET

Security classification of this page: Unclassified

1. Document Numbers
   (a) AR Number:
   AR-002-290
   (b) Document Series and Number:
   Aerodynamics Note 402
   (c) Report Number:
   ARL-AERO-NOTE-402

2. Security Classification
   (a) Complete document:
   Unclassified
   (b) Title in isolation:
   Unclassified
   (c) Summary in isolation:
   Unclassified

3. Title: A ROTOR WAKE MODEL FOR FORWARD FLIGHT SIMULATION STUDIES

4. Personal Author:
   Reddy, K. R.

5. Document Date:
   June, 1981

6. Type of Report and Period Covered:

7. Corporate Author(s):
   Aeronautical Research Laboratories.

8. Reference Numbers
   (a) Task:
   (b) Sponsoring Agency:

9. Cost Code:
   51 7740

10. Imprint:
    Aeronautical Research Laboratories, Melbourne

11. Computer Program(s)
    (Title(s) and language(s)):

12. Release Limitations (of the document): Approved for Public Release

12-0. Overseas:	N.O.		P.R.	1	A		B		C		D		E	

13. Announcement Limitations (of the information on this page):
    No Limitation

14. Descriptors:
    Rotor wakes
    Helicopter flight simulation
    Rotary-wing aerodynamics
    Computerized simulation
    Vortices
    Downwash
    Mathematical models

15. Cosati Codes:
    0102

16. *ABSTRACT*

This Note presents an attempt to develop a rotor wake model for forward flight which requires only modest computing time and, therefore, is suitable for flight simulation studies. Free and rigid wake models are discussed, together with various simplifying assumptions, in order to reduce the computation time to acceptable levels for simulation studies. Using a tip vortex wake model and the Biot-Savart relation, induced velocities are calculated in the rotor plane. It is then assumed that the tip vortex wake takes the form of a skewed helix. Such a simple prescribed model requires little computing time and the accuracy of its results when compared with more elaborate free wake models shows considerable promise.

CONTENTS

NOTATION

a_{ij}	Core size of the vortex element *ij*
L_{ij}	Length of the vortex element *ij*
r	Radial distance from the rotor hub
r_i, r_j	Distances of the point *P* from the end points of the vortex element *ij* as shown in Figure 6
R	Outer radius of the rotor
v_i	Induced velocity
v_x, v_y, v_z	Velocity components in *x*, *y*, and *z* direction respectively
$x\ y\ z$	The cartesian co-ordinate system
x_p, y_p, z_p	Co-ordinates of the point *P*
α_T	Tip-path-plane angle
Γ_{ij}	Vortex strength of the element *ij*
μ	Advance ratio
ψ	Azimuth angle
Ω	Rotational speed of the rotor blade

1. INTRODUCTION

In flight simulation studies, the forces and moments acting on a helicopter rotor blade are often estimated on the assumption that the distribution of induced velocity over the disc is uniform. Experimental studies have revealed, however, that the assumption is not well founded, especially in forward flight. The only justification for using the uniform inflow distribution is that the calculations are simple and the results obtained using this assumption are in fair agreement with experimental data. Since the theory gives reasonable average rotor thrust, blade loads and moments, it can be used satisfactorily as a first approximation in rotor performance and flight simulation calculations. However, to obtain a more fundamental picture of the mechanism of rotor induced flow, analysis of the rotor vortex wake[1] must be considered. Though it has been recognized for many years that the detailed structure of the rotor downwash could have a substantial influence on rotor characteristics such as performance and blade flapping motion, early efforts at computation of the induced flow in forward flight were limited in utility because it was impracticable to account for individual blades. The advent of the high-speed electronic digital computer has made possible the straightforward approach of tracing the vortex filaments trailed by each blade, and using the Biot–Savart relation to obtain velocities.

In the following sections wake models, both free and prescribed, are discussed, together with various simplifying assumptions to reduce the computational time required. The computational procedure to calculate the induced velocity due to vortex elements is also discussed. It is concluded that even with modern fast computers the computational time greatly restricts the application of the free wake model. On the other hand it is shown that a simple tip vortex model which is assumed to take the form of a skewed helix gives satisfactory accuracy, compared with the more complex free wake model. It is considered that a simple prescribed rotor wake model for forward flight is substantially in accordance with the true state of the flow generated by a rotor blade and allows downwash calculations, with acceptable computing time, for flight simulation studies.

2. THE VORTEX WAKE MODEL FOR FORWARD FLIGHT

Consider the rotor blade in steady forward flight.[1] Because the circulation generally varies along the span, vortex lines leave the trailing edge and spiral downwards beneath the rotor. In addition, however, the blade experiences oscillatory aerodynamic effects even in steady forward flight. This is fundamental for rotary wings since variations in relative airspeed occur at each blade section as the blade rotates. Flapping and blade pitch angles are made to vary with azimuth in order to tilt the rotor thrust vector in the desired direction. Hence the blade incidence varies as a function of rotor azimuth, creating shed vortices in the wake. Thus as the blades rotate, a continuous sheet of shed and trailing vorticity streams from each section of the blade as shown in Figure 1. Similar wake structures exist for other blades, with the aggregate forming the complete wake. This system of vortex wake is the one which makes the helicopter aerodynamic analysis so much more complicated than the fixed wing aerodynamic problem. Whereas for the fixed wing the wake is assumed to lie in the same plane as the wing, the helicopter wake is blown below the plane of the rotor. The exact configuration of the vortex wake depends on the local velocity, which is the sum of the induced velocity and the main flow due to helicopter motion. Since the resultant local velocity is determined in part by the spatial distribution of the wake vorticity, a closed form analytic solution for both the downwash and wake vorticity is virtually impossible. Hence numerical methods must be used to solve the problem.

A detailed wake model for calculating the induced velocity would represent the rotor blades by lifting surfaces and the rotor wake by vortex sheets. The calculation of wake geometry would involve the computation of the distortion and roll-up of these vortex sheets due to their own induced velocities and those of the lifting surfaces. As the vortex sheets roll up into line vortices, viscous effects would become important in the vortex core.[2] Because the above model would require an excessive amount of CPU time, a simplified model must be constructed. For mathematical analysis, the rotor blades are represented by lifting lines (bound vortices), and the vortex wake (shown in Fig. 1) is idealized by a set of trailing and shed line vortices as shown in Figure 2. The trailing vortex lines are trailed aft along streamlines relative to the rotor blade while the shed vortex lines are shed parallel to the instantaneous position of the rotor blade. These vortex filaments are free to convect at the local velocity, which is the sum of the free stream velocity and the velocity induced by the trailing, shed, and bound vortices. This form of rotor wake representation is one of the most complex. The computer requirements and cost to run such a wake model are normally prohibitive. This point will be very clear later when some results for a much simplified version of this model are presented. Comparisons of entire wake flows predicted using this (refer Fig. 2) wake model with experimental measurements have indicated that use of a coarse mesh resulted in poor induced velocity predictions, and that use of a fine mesh increased running time to an unacceptable level.[3,4] Therefore, the full mesh wake was used[4] to represent the wake immediately behind the blades, and a modified wake model was used in the remainder of the wake, as shown in Figure 3. The modified wake consists of trailing vortices only. It is known from experiments that the strength of the shed vorticity is small in comparison to the trailing vorticity. Hence the influence of the shed vorticity on the wake distortions is neglected. The locations, circulations, and core sizes of the trailing vortices in the modified wake are determined in terms of the final values of the full mesh wake. The wake induced velocities, wake distortions, and other calculations are essentially the same for both the full mesh wake and for the modified wake portions of the wake model. Piziali[5] used the above model in his rigid wake analysis. Clark and Leiper,[6] Landgrebe,[4] and Sadler[3] used a similar vortex model in their free wake analyses. Although this wake model, when used in free wake analysis, gives results which show good agreement with experimental results, the large computational time required limits its use, thus necessitating further simplification.

A further simplification of the rotor wake geometry is valid if certain approximations based on experimental results are introduced. It is known that the vorticity trailed by a rotor blade tends to be concentrated towards the blade tip and rolls up into a core of rotating air (see Ref. 17). Most of the contribution to induced velocity and blade loading comes from this tip vortex. Representation of the real wake by a tip vortex alone is a fairly good approximation.[7] This wake model is shown in Figure 4. Crimi[7] and Scully[8] used similar idealized wake models. In Figure 4, it is indicated that the vorticity which rolls up into the tip vortex must clearly be shed as a sheet; however, little is known about the roll-up process. Flow visualization pictures suggest that roll-up occurs close to the blade. In this paper it is assumed that the roll-up takes place immediately behind the blade trailing edge, that is, it is assumed that the vortex sheet roll-up angle (see Fig. 4) is zero.

3. COMPUTATIONAL PROCEDURE TO CALCULATE THE INDUCED VELOCITY DUE TO VORTEX ELEMENTS

In the previous section, a simplified model was evolved for the vortex wake of a rotor blade. The next task is to determine the geometrical distribution of the vorticity in the flow field. The wake geometry is calculated by an iterative numerical process. As a part of the computational procedure, the tip vortex behind each blade is broken into convenient straight line segments as shown in Figure 5. These segments were chosen to be sufficiently small so that for purposes of computation of the wake-induced velocities they may be considered as rectilinear vortices having constant circulation along their length. The wake configuration at any instant is then defined by the location of these line segments. Each vortex filament has length L_{ij}, core radius a_{ij}, and vortex strength Γ_{ij}. The length of each vortex element depends on how finely the tip vortex is divided. The wake and bound vortices are assumed to have finite-sized cores of rotational fluid. Various sources[7,8] estimate the vortex core radius and give a range of values. However, for the case of a rotor in forward flight, the results turn out to be very insensitive to vortex core size. After extensive calculations, Crimi[7] assigns a representative value of 0·05 to the ratio of core radius to the rotor radius. The vortex strength Γ_{ij} of the filament is taken as the value of the bound vorticity when it was generated. Once formed, the strength of the vortex elements are assumed to remain unchanged as the wake develops. Knowing the vortex filament length, core radius, and strength, the Biot–Savart relation can be used to calculate the induced velocity at any point. Figure 6 shows a typical vortex element between the points *i* and *j*. Using cartesian co-ordinates, the induced velocity components due to this vortex filament are denoted by v_x, v_y, and v_z in the *x*, *y* and *z* direction respectively. The method for calculating these induced velocities using the Biot–Savart relation is well known.[3,4,7] For completeness, the formulae are given in Appendix A. However, these formulae are not useful when it is necessary to calculate the induced velocity at certain important points in the flow field.

For the case of calculating the velocity induced at a point on the tip vortex by the two immediately adjacent vortex segments, the use of the straight line vortex segments is inadequate, since it would give zero induced velocity at the point due to these two vortex segments. The two vortex segments adjacent to the point are therefore replaced by a circular arc vortex segment passing through the three points determined by the ends of the vortex segments. The velocity induced at a point by the circular arc vortex segment is given in References 3 and 7.

Other potentially awkward aspects of using concentrated line vortices arise when it is attempted to compute the induced velocity very close to a vortex filament. For this case, the effects of a finite vortex core, where viscosity becomes important and the Biot–Savart relation no longer applies directly should be included. A useful first approximation to the induced velocity inside a vortex core is to assume solid body rotation of the vortex core with an induced velocity at the outer edge of the vortex core equal to the result given by the Biot–Savart relation at that point.[3] Thus for most cases it isonly necessary to check whether or not the point at which the induced velocity must be calculated is inside the vortex core, and apply either the Biot–Savart relation or the solid body rotation model.

4. FREE WAKE METHOD

In the free wake method the computations are initiated by specifying the initial wake configuration. The velocity contributions of all vortex elements are calculated at each reference point (end points of vortex filaments). Then these points are allowed to propagate with the computed velocity generating a new vortex geometry. This process is repeated until a wake is generated which is unchanged from one iteration to the next. This wake is taken as the equilibrium form and is used in rotor downwash calculations.

As an example the rotor wake for a four-bladed Wessex rotor is shown in Figure 7. The important parameters for the rotor are:

Advance ratio	0·215
Rotor forward tilt	3·5 deg
Rotor speed	22·2 rad/s
Weight	53 400 N
Rotor radius	3·5 m

The iterative vortex wake solution converges for this case. It takes 36 minutes CPU time on the PDP DEC 10 system. For clarity, the tip vortex of only one of the blades is presented in Figure 7. The wake elements become distorted as a result of interactions with other elements in the wake. The large displacements of the wake elements two to three rotor radii downstream must be viewed with caution considering stability and viscous dissipation problems involved in that region and beyond. These large downstream distortions, however, do not significantly influence the flow field at the rotor where rotor downwash calculations are needed in performance computations.

Using the converged wake, the induced velocity can be calculated at any reference point, again applying the Biot–Savart relation. Time averaged induced velocities at various points in the rotor plane were calculated for this case (refer Fig. 11). These results are discussed in detail in succeeding sections.

In the free wake method, the computational procedure is fundamentally an iterative process. Induced velocities at wake reference points are calculated using the previously calculated wake geometry and then these points are allowed to propagate to constitute the new wake geometry. The process is repeated until convergence.

The converged wake is the one which exists in force-free equilibrium[6] and the aim is to find the arrangement of the vortex segments in space which will satisfy this condition. This presents a formidable computational problem since every vortex segment is influenced by, and influences, every other segment.

Even using modern, fast computing machines, the time required in the free wake analysis restricts its application. For example, depending on the advance ratio, 4 to 10 iterations may be needed in the rotor wake geometry calculation. This means 30 to 50 minutes CPU time on the PDP DEC 10 system. The lower the advance ratio, the more time is required for wake vortex interaction. Thus in rotor downwash calculations, the major portion of the computer time goes into the determination of the wake geometry.

5. RIGID WAKE METHOD

If the wake geometry can be prescribed, based on previous theoretical calculations and experimental result, much time and labour can be saved. This is particularly necessary where induced downwash calculations form a part of the overall problem of helicopter flight simulation studies. For flight simulation the overall mathematical model is divided into simple realistic sections (e.g. rotor aerodynamics, fuselage aerodynamics, helicopter control system, dynamics of slung bodies) so that the problem can be accommodated on a medium-sized computer and results expected in a reasonable time. With this application in view the various simple prescribed wake methods described here are studied and the accuracy of their results determined by comparing with the results of the free wake model.

The concept of the prescribed wake method is simple. In the rotor wake, the vortex filaments are distributed in some complex form as shown in Figure 7. This has to be arranged into a simple logical form so that it closely approximates the actual rotor wake. Willmer[9] and Loewy[10] used infinite line vortices to represent the prescribed wake. Coleman *et al.*,[11] and Heyson and Katzoff[12] used a simple pattern consisting of circles and straight lines. Piziali,[5] and Kocurek and Tangler[13] used a method in which the vortex filaments, both shed and trailing, are broken into a number of straight elements, so that the wake has the appearance of a twisted spider's web. Cook[14] used circular vortex rings and ring segments to represent the vortex wake in forward flight downwash calculations. Recently, Rayner[15,16] used circular rings to study the hovering flight of birds and insects, and elliptical rings to generate the wake of the forward flight of animals. This interesting work could be classified as a semi-rigid wake model.

The decomposition of the spiral trailing vortex filaments into simple circular elements for the helicopter flight may be easily demonstrated. In Figure 8, the spiral trailing tip vortex filaments are traced as they are generated by a four-bladed advancing rotor (see Ref. 18).

Considering the first section of tip vortex from the blade 2, it could easily be approximated to a semi-circular element. Furthermore, the contributions of additional spirals may be approximated to complete circles. On this basis, Cook developed a prescribed model as shown in Figure 9. Results obtained by Cook using this model are also presented in Figure 11. Although the geometric differences between the distorted (Fig. 7) and undistorted (Fig. 9) wakes are significant, it has been found[1] that the differences are generally unimportant when it comes to the determination of rotor downwash for conventional forward flight conditions. This cannot be generalized, however, to include flight conditions which place portions of the wake in the plane of the rotor, for example during manoeuvres.

The hovering rotor generates approximately a quarter to a third of its lift over the outer 10% of the blades. The passage of a tip vortex close to the blade in this tip region has been shown[1] to influence significantly the blade tip loading. In forward flight with forward tilt of the rotor disc, the blades are moving away from the wake, and therefore are less influenced by it. The vortices do not pass continuously under the blades in the predominant loading regions. In fact, for rotors with a small number of blades flying at high advance ratios, there are no blade-vortex interactions over a large range of the blade azimuth travel. This makes the rigid wake model a fair proposition in forward flight simulation.

As stated earlier, the main aim of the work reported here is to develop a rotor wake model so that downwash calculations can be made in a few minutes of computer time. If interest is limited to calculating the velocity field in the rotor plane a simple vortex wake geometry, in the form of a skewed helix, can be used in combination with the Biot-Savart relation to produce a satisfactory, simple model. The results from this model are compared with those of Cook and free wake calculations to assess their accuracy. From Figures 7 and 10 it is clear that the skewed helix closely represents the free wake near the rotor but that it differs increasingly, from the free wake, with distance below the rotor plane. However, this divergence is not important since the vortex elements far away from the rotor contribute very little to the induced velocity. The reason for this is that the induced velocity calculated at a point by the Biot–Savart relation is inversely proportional to its distance from the vortex element. The formulae for calculating the wake geometry are given in Appendix B. Induced velocities calculated using the prescribed wake model are also presented in Figure 11, for the Wessex rotor, again for the same operating conditions.

Figure 11 shows the time-averaged induced velocities in the rotor plane calculated using free vortex and prescribed helical wake models, along with Cook's circular ring vortex model. Glauert's classical trapezoidal downwash distribution is also presented in the figure. Induced velocity as a function of blade span is shown at 12 azimuth stations. The graphs illustrate the magnitude of the difference between various approaches and show that the basic agreement between the free vortex and prescribed helical wake induced velocity results is fair. The characteristic upwash at the front of the rotor disc is well defined. By far the largest difference between the free vortex and prescribed helical wake results is at an azimuth angle of 300°.

With Cook's vortex ring model, over the front half of the rotor disc, the amplitude of the induced velocity fluctuates along the blade span. These fluctuations are, however, not observed in the results calculated here using the free vortex and prescribed helical wake models.

6. CONCLUDING REMARKS

A number of mathematical models for calculation of rotor downwash in forward flight has been investigated. It is found that even the tip vortex model in free wake analysis requires about 50 minutes CPU time on a PDP DEC 10 for the Wessex helicopter. For flight simulation studies this amount of computer time is unacceptable. Various ways to reduce the time are being investigated. The most useful approach for practical applications seems to be an empirical one based on a prescribed wake type of approximation. The development of a satisfactory method requires the knowledge of what kind of wake geometries occur under various flight conditions. This in turn can only be acquired by the extensive analysis of rotor wake experimental data, theoretical results, and physical reasoning. Preliminary results carried out using a simple skewed helix model are very encouraging.

7. ACKNOWLEDGMENTS

The author is indebted to Dr. G. D. Mallinson for use of his graphics computer programs.

REFERENCES

1. Landgrebe, A. J., and Cheney, M. C. Rotor Wakes—Key to Performance Prediction. AGARD Conference Proceedings, Aerodynamics of Rotary Wings, AGARD-CP-110, France, September 1972.
2. Van Holten, T. H. On the Validity of Lifting Line Concepts in Rotor Analysis. *VERTICA*, Vol. 1, 1977, pp. 239-254.
3. Sadler, S. G. Development and Application of a Method for Predicting Rotor Free Wake Positions and Resulting Rotor Blade Air Loads. NASA CR-1911, December 1971.
4. Landgrebe, A. J. Analytical Methods for Predicting Rotor Wake Geometry. *JAHS*, Vol. 41, October 1969, pp. 20-32.
5. Piziali, R. A. Method for the Solution of the Aeroelastic Response Problem for Rotating Wings. *J. Sound and Vibration*, Vol. 4, 1966, pp. 445-489.
6. Clark, D. R., and Leiper, A. C. The Free Wake Analysis—A Method for the Prediction of Helicopter Rotor Hovering Performance. *JAHS*, Vol. 15, January 1970, pp. 3-11.
7. Crimi, P. Theoretical Prediction of the Flow in the Wake of a Helicopter Rotor. Cornell Aero. Lab. Report No. BB-1994-S-1, September 1965.
8. Scully, M. P. A Method of Computing Helicopter Vortex Wake Distribution. MIT Report No. ASRL TR 138-1, June 1967.
9. Willmer, M. A. P. The Loading of Helicopter Blades in Forward Flight. Rep. Memo. Aero. Res. Coun. 3318, 1959.
10. Loewy, R. G. A Two-dimensional Approach to the Unsteady Aerodynamics of Rotary Wings. *J. Aeronautical Sci.*, Vol. 24, 1957, pp. 81-93.
11. Coleman, R. P., Feingold, A. M., and Stempin, C. W. Evaluation of the Induced Velocity Field of an Idealized Helicopter Rotor. NACA Wartime Report, ARR-L5E10, June 1945.
12. Heyson, H. H., and Katzoff, S. Induced Velocities Near a Lifting Rotor with Non-uniform Disc Loading. NACA Rep. 1319, 1958.
13. Kocurek, J. D., and Tangler, J. L. A Prescribed Wake Lifting Surface Hover Performance Analysis. 32nd National V/STOL Forum, AHS, Washington, D.C., May 1976.
14. Cook, C. V. Induced Flow Through a Helicopter Rotor in Forward Flight. Westland Helicopters Limited, Research Paper 374, January 1970.
15. Rayner, J. M. V. A Vortex Theory of Animal Flight. Part 1. The Vortex Wake of a Hovering Animal. *J. Fluid Mech.*, Vol. 91, 1979, pp. 697-730.
16. Rayner, J. M. V. A Vortex Theory of Animal Flight. Part 2. The Forward Flight of Birds. *J. Fluid Mech.*, Vol. 91, 1979, pp. 731-763.
17. Saunders, G. H. Dynamics of Helicopter Flight. John Wiley & Sons, New York, 1975.
18. Davenport, F. J. Aerodynamic Characteristics of a Model Helicopter Rotor Operating Under Nominally Stalled Conditions in Forward Flight. *JAHS*, Vol. 9, 1964, pp. 26-33.

APPENDIX A

Let i and j be the end points of a straight line vortex filament and P be the point at which the induced velocity is to be computed. These three points can be arbitrarily oriented in space as shown in Figure 6. The induced velocity components v_x, v_y, and v_z at P due to the vortex element Γ_{ij} are given by the Biot–Savart relations:[4,5]

$$v_x = \frac{\Gamma_{ij}}{4\pi} C[(y_p - y_i)(z_p - z_j) - (z_p - z_i)(y_p - y_j)]$$

$$v_y = \frac{\Gamma_{ij}}{4\pi} C[(z_p - z_i)(x_p - x_j) - (x_p - x_i)(z_p - z_j)]$$

$$v_z = \frac{\Gamma_{ij}}{4\pi} C[(x_p - x_i)(y_p - y_j) - (y_p - y_i)(x_p - x_j)]$$

where

$$C = \frac{1}{R} \frac{(r_i + r_j)}{r_i r_j (r_i r_j + C_1 + C_2 + C_3)}$$

$$C_1 = (x_p - x_i)(x_p - x_j)$$

$$C_2 = (y_p - y_i)(y_p - y_j)$$

$$C_3 = (z_p - z_i)(z_p - z_j)$$

$$r_i = [(x_p - x_i)^2 + (y_p - y_i)^2 + (z_p - z_i)^2]^{1/2}$$

$$r_j = [(x_p - x_j)^2 + (y_p - y_j)^2 + (z_p - z_j)^2]^{1/2}$$

APPENDIX B

Co-ordinates of the skew helix wake reference point P_{ij} (refer Fig. 5) are calculated using the following formulae:[3,5,7]

$$x(i,j) = \cos\left[\psi + (j-1)\frac{2\pi}{N_B} - (i-1)\Delta\psi\right] + (i-1)\Delta\psi\mu\cos\alpha_T$$

$$y(i,j) = \sin\left[\psi + (j-1)\frac{2\pi}{N_B} - (i-1)\Delta\psi\right]$$

$$z(i,j) = -(i-1)\Delta\psi\left[\mu\sin\alpha_T + \left(\frac{N_B}{2}\frac{W}{\pi^2 N_B \rho \Omega^2 R^4}\right)^{1/2}\right]$$

where ψ = Azimuth angle as shown in Figure 5

N_B = Number of blades

μ = Advance ratio

α_T = Blade tip-path-plane angle as shown in Figure 5

$\Delta\psi$ = Angle $(2\pi/N_A)$; N_A being the number of azimuth stations into which rotor plane is divided

W = Weight of the rotorcraft

ρ = Air density

Ω = Rotor angular speed

R = Rotor radius

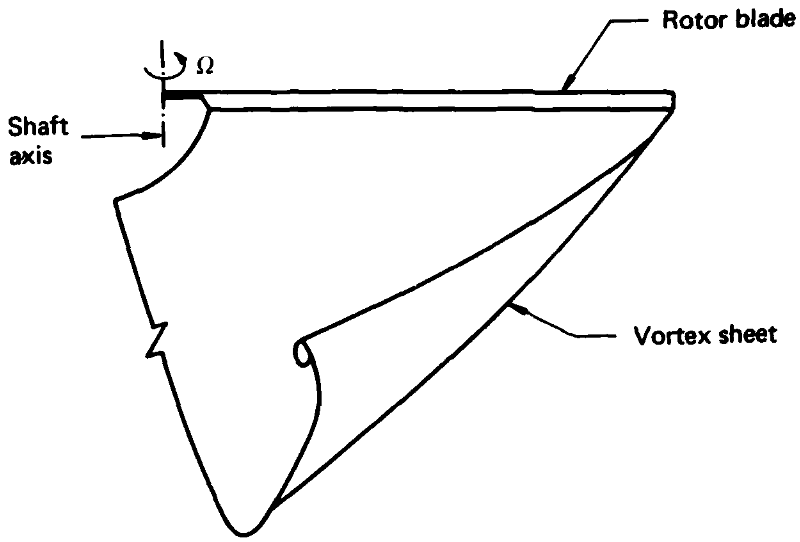

FIG. 1 ROTOR BLADE WAKE STRUCTURE – REAL FLOW

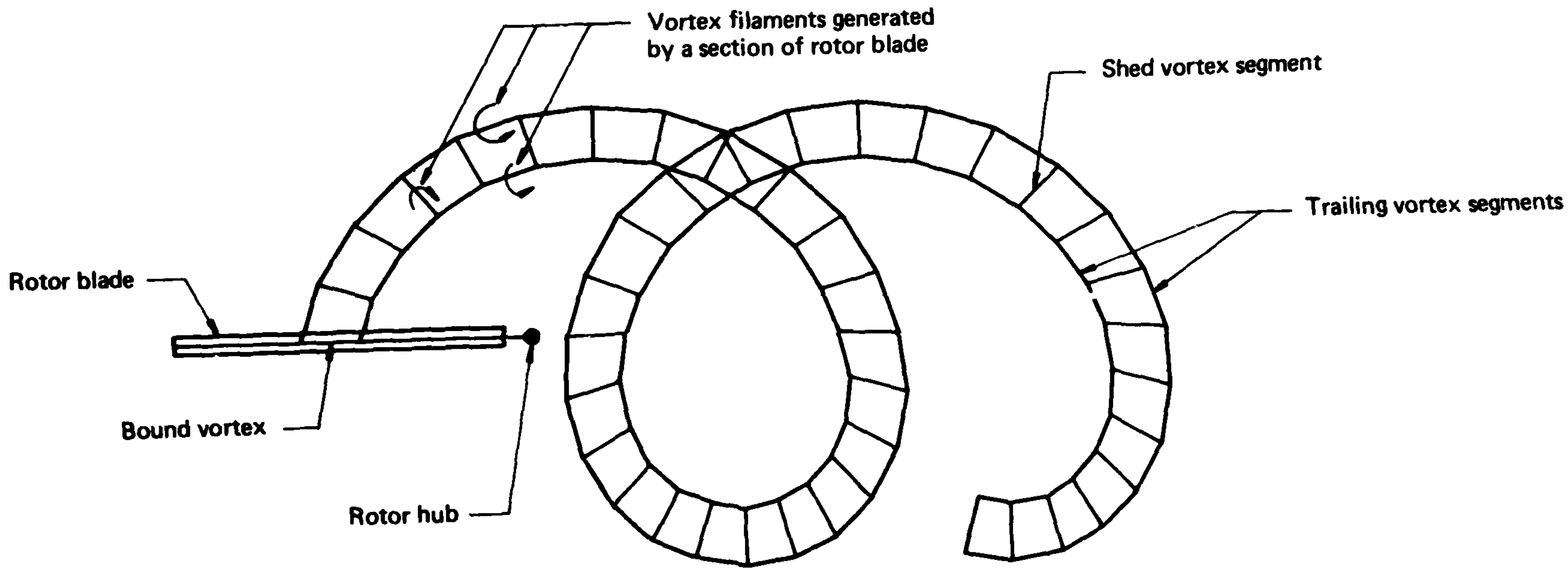

FIG. 2 ROTOR WAKE STRUCTURE – IDEALIZED LINE VORTEX MODEL

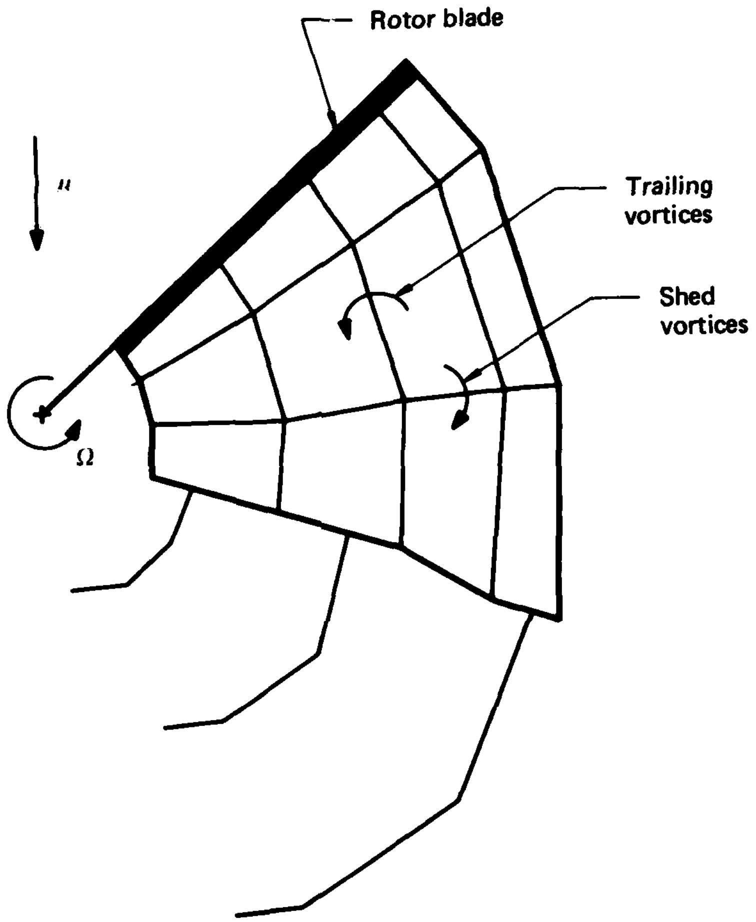

FIG. 3 COMPLEX NEAR WAKE AND MODIFIED SIMPLE FAR WAKE

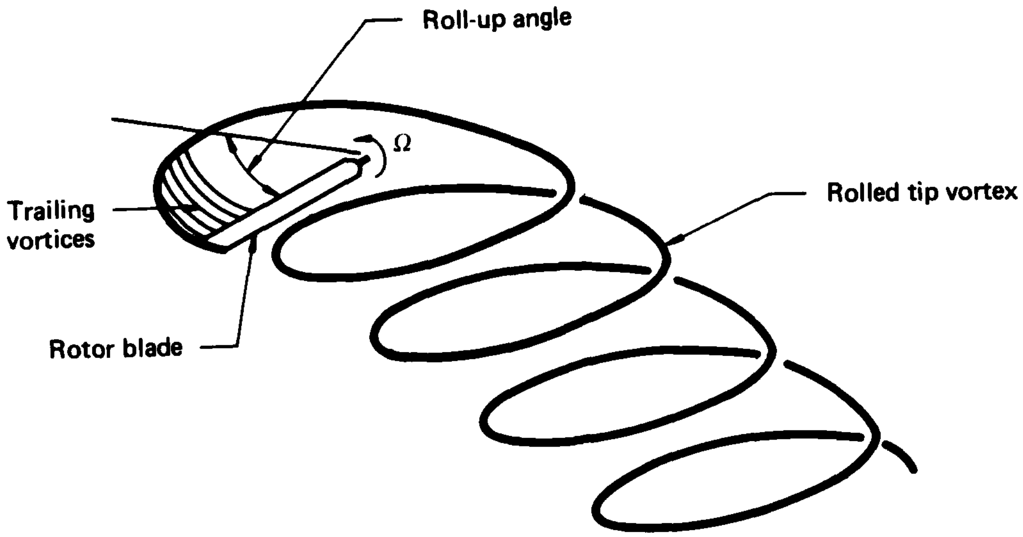

FIG. 4 ROLL-UP OF TRAILING VORTICES

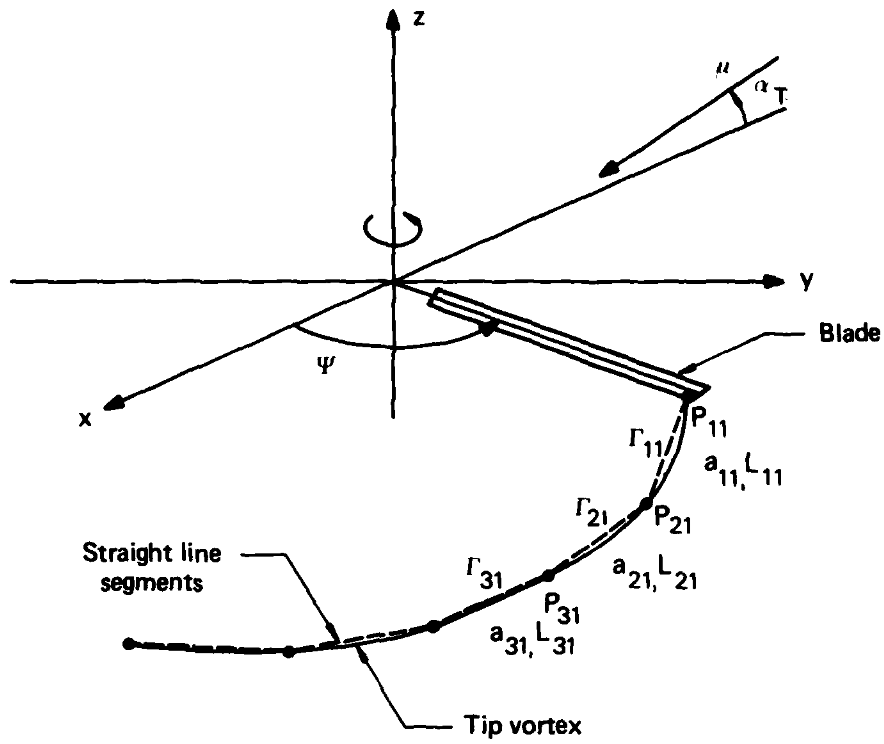

FIG. 5 A TYPICAL TIP VORTEX GENERATED BY A ROTATING BLADE

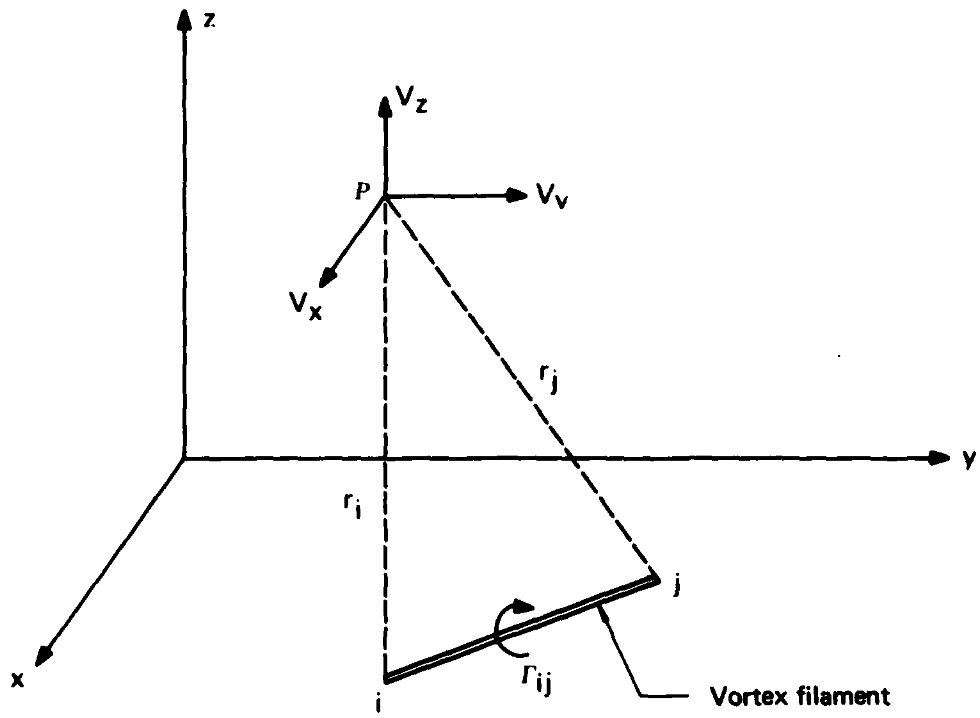

FIG. 6 FLOW INDUCED BY A VORTEX ELEMENT

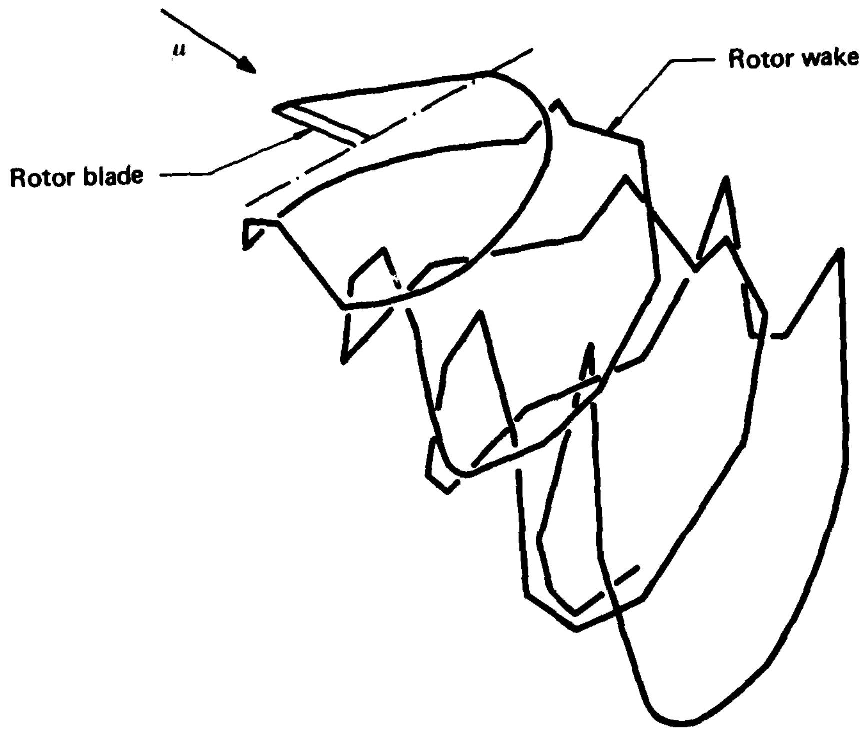

FIG. 7 DISTORTED WAKE BELOW THE ROTOR AFTER THE CONVERGENCE OF THE FREE WAKE SOLUTION

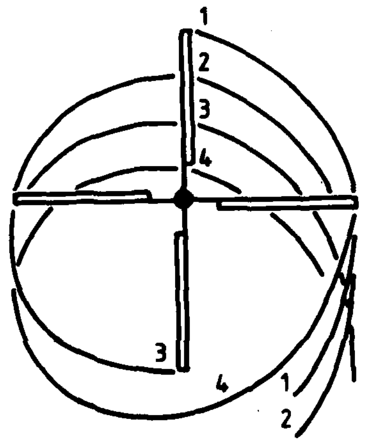

FIG. 8 TIP VORTEX GEOMETRY FOR A FOUR BLADED ROTOR

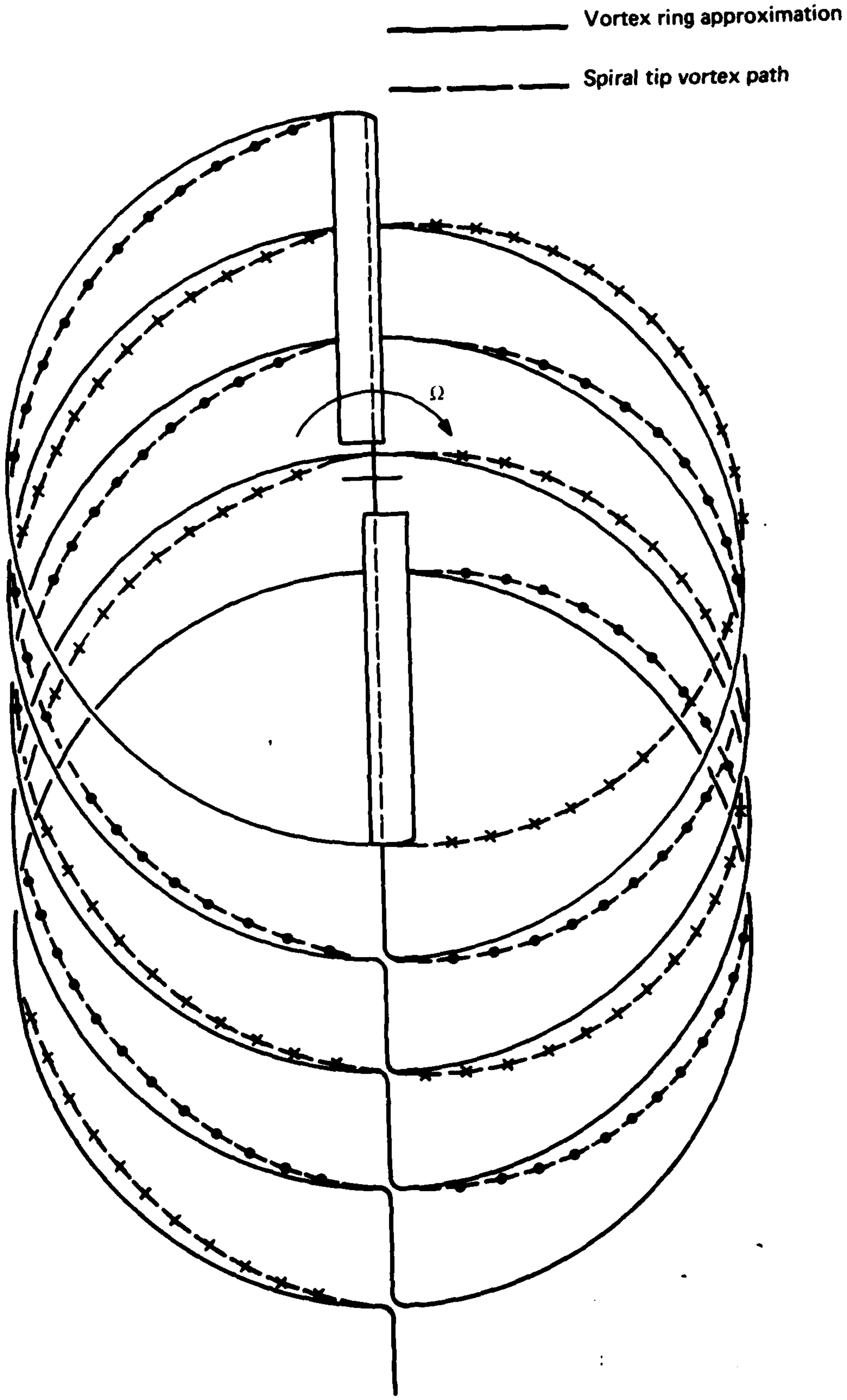

FIG. 9 COOK'S VORTEX RING MODEL

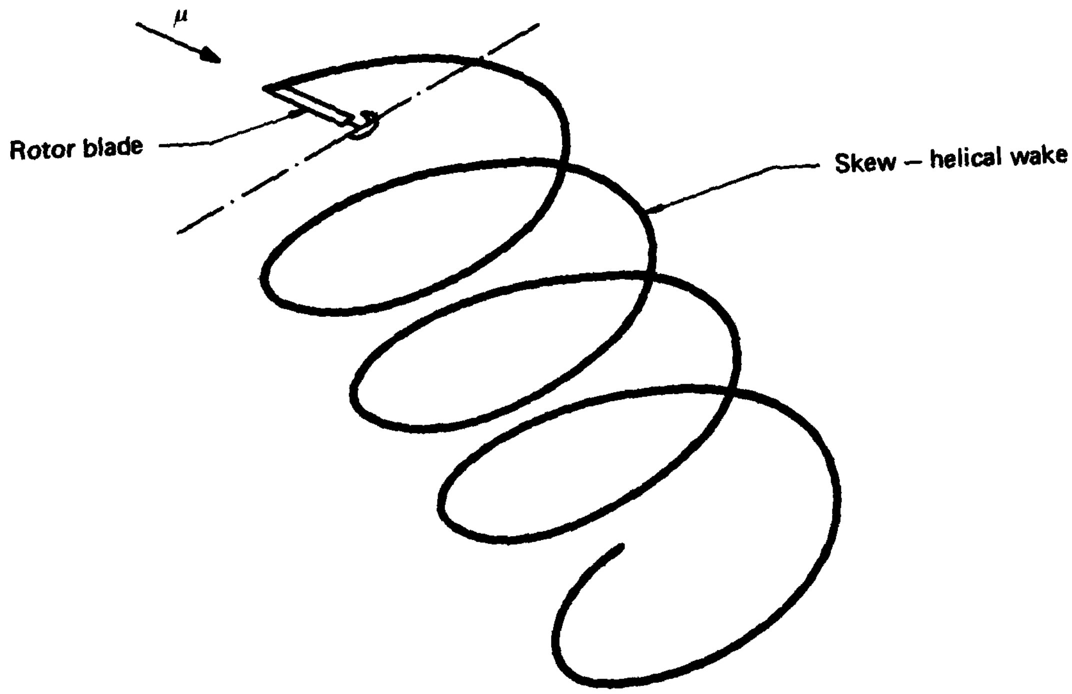

FIG. 10 PRESCRIBED SKEW-HELICAL WAKE CONFIGURATION

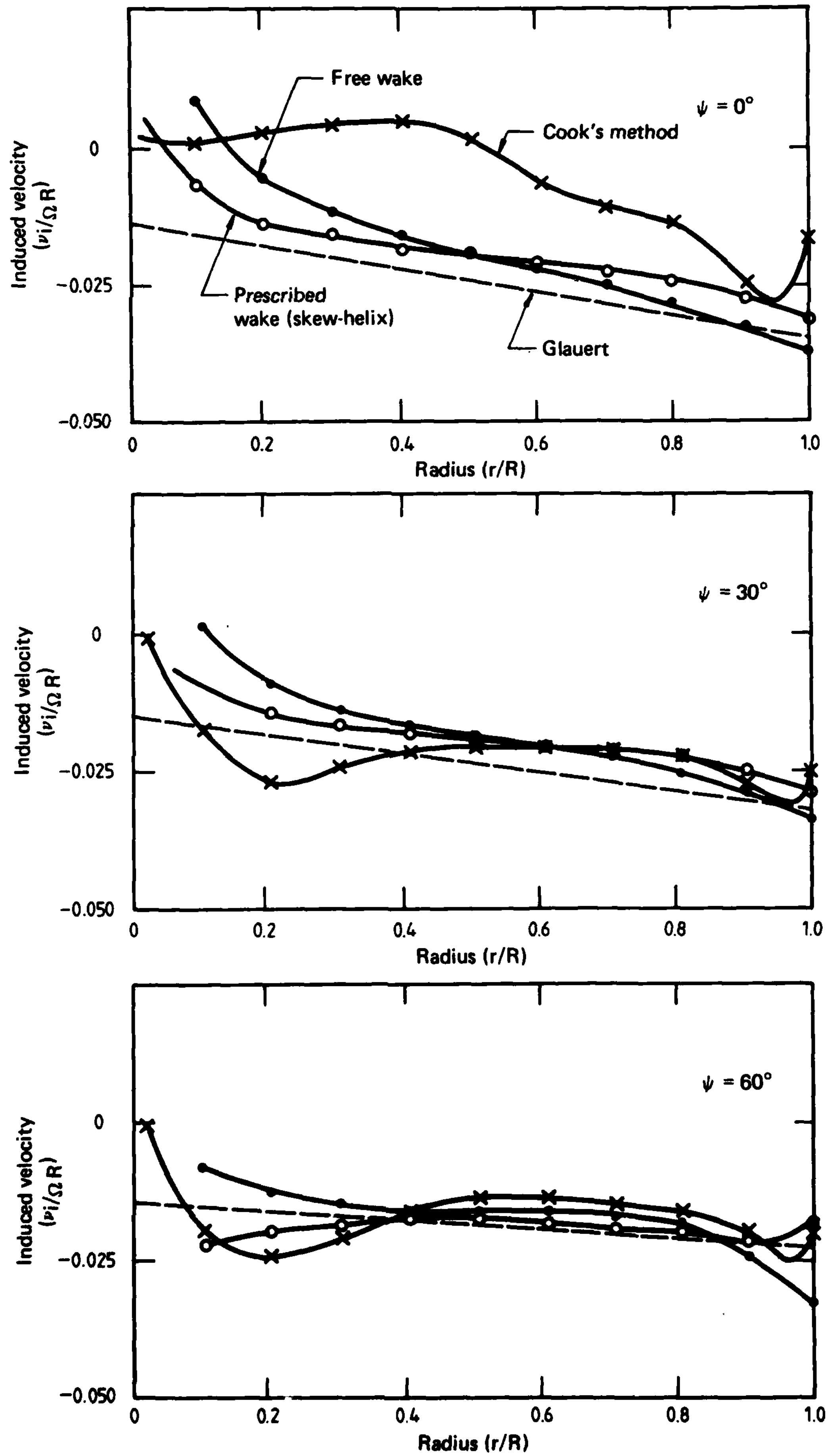

FIG. 11 VARIATION OF INDUCED VELOCITY WITH ROTOR RADIUS

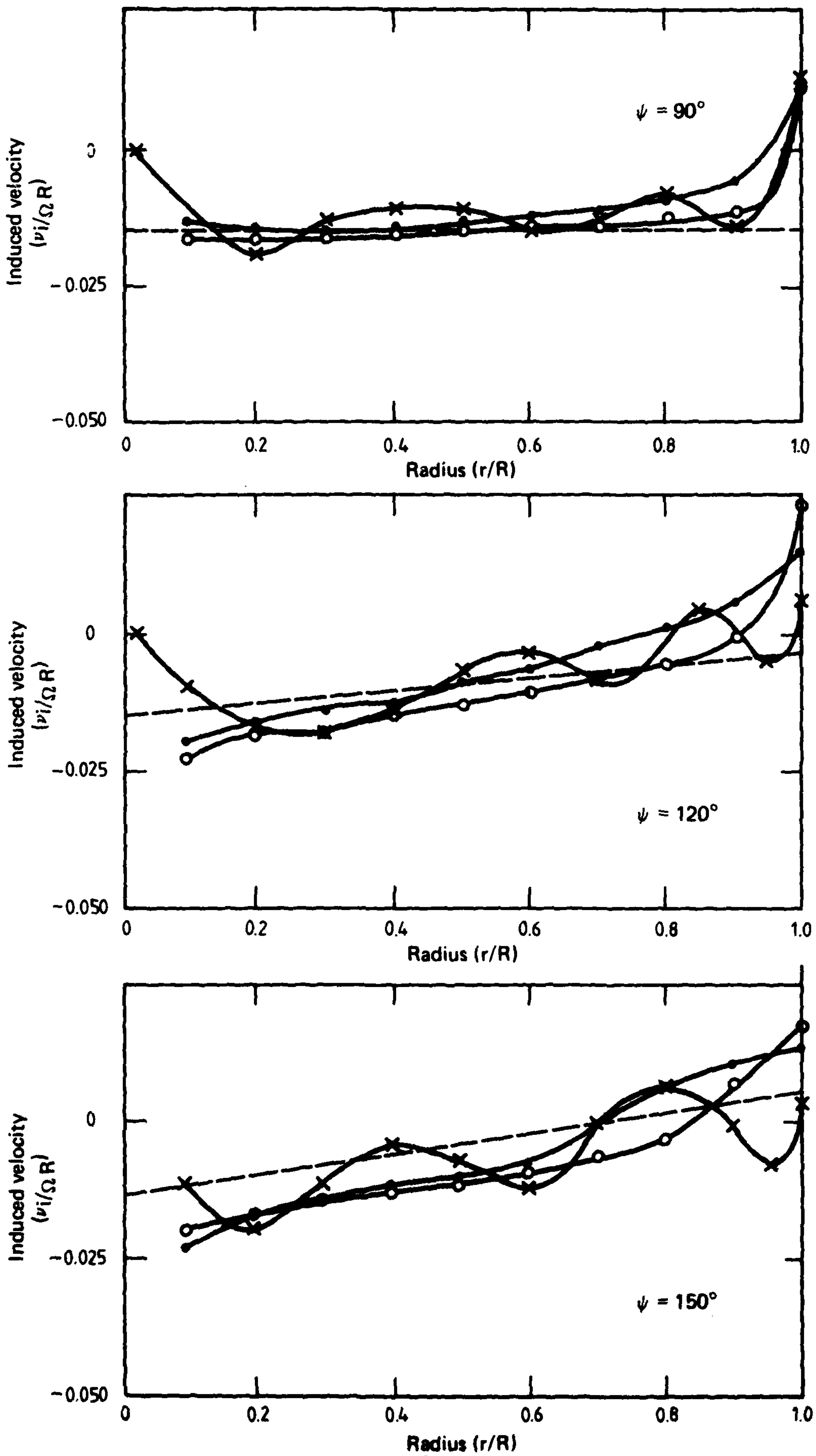
ψ = 90°
Induced velocity ($\nu_i/\Omega R$)
0
−0.025
−0.050
0
0.2
0.4
0.6
0.8
1.0
Radius (r/R)
ψ = 120°
Induced velocity ($\nu_i/\Omega R$)
0
−0.025
−0.050
0
0.2
0.4
0.6
0.8
1.0
Radius (r/R)
ψ = 150°
Induced velocity ($\nu_i/\Omega R$)
0
−0.025
−0.050
0
0.2
0.4
0.6
0.8
1.0
Radius (r/R)
FIG. 11 (CONT)

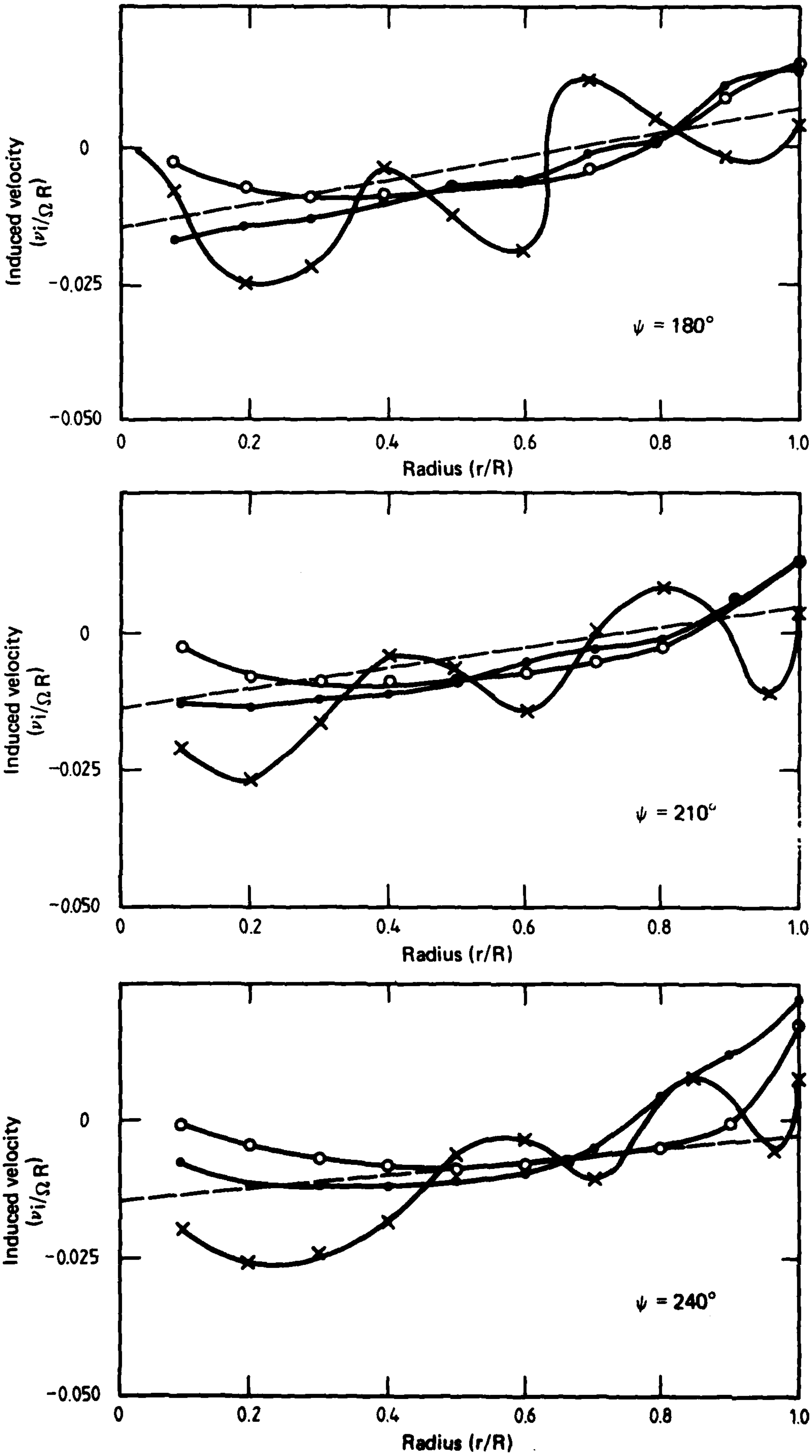
Induced velocity ($\nu_i/\Omega R$)
0
-0.025
-0.050
0
0.2
0.4
0.6
0.8
1.0
Radius (r/R)
ψ = 180°
Induced velocity ($\nu_i/\Omega R$)
0
-0.025
-0.050
0
0.2
0.4
0.6
0.8
1.0
Radius (r/R)
ψ = 210°
Induced velocity ($\nu_i/\Omega R$)
0
-0.025
-0.050
0
0.2
0.4
0.6
0.8
1.0
Radius (r/R)
ψ = 240°

FIG. 11 (CONT)

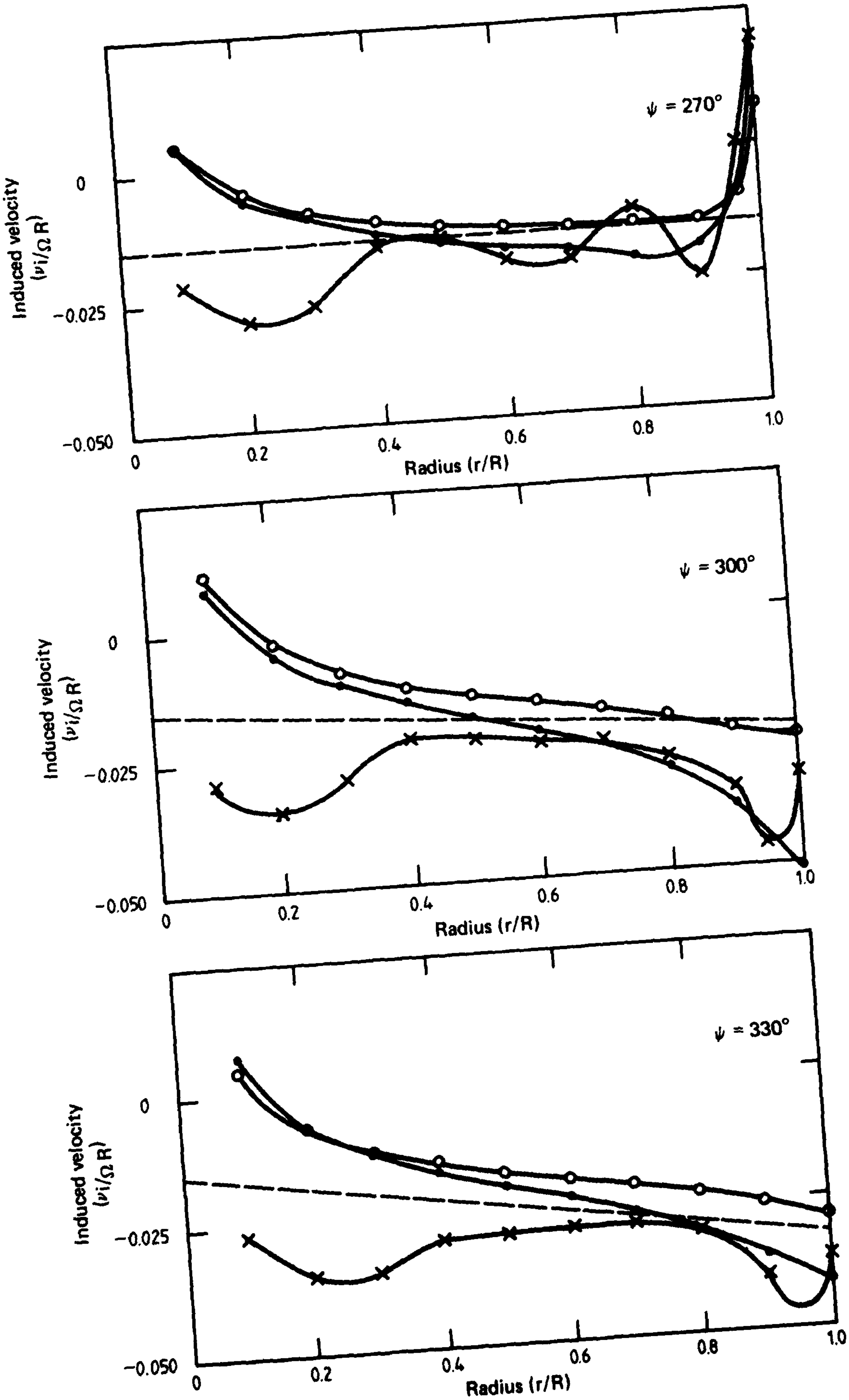
ψ = 270°
ψ = 300°
ψ = 330°
Induced velocity ($\nu_i/\Omega R$)
0
−0.025
−0.050
0
0.2
0.4
0.6
0.8
1.0
Radius (r/R)

FIG. 11 (CONT)

DISTRIBUTION

	Copy No.
AUSTRALIA	
Department of Defence	
Central Office	
Chief Defence Scientist	1
Deputy Chief Defence Scientist	2
Superintendent, Science and Technology Programmes	3
Australian Defence Scientific and Technical Representative (UK)	—
Counsellor, Defence Science (USA)	—
Defence Central Library	4
Document Exchange Centre, DISB	5–22
Joint Intelligence Organization	23
Aeronautical Research Laboratories	
Chief Superintendent	24
Library	25
Superintendent Aerodynamics	26
Divisional File—Aerodynamics	27
Author: K. R. Reddy	28
Aerophysics Group (D. C. Collis)	29
TTCP HTP–6 National Leader (D. C. Collis)	30
Materials Research Laboratories	
Library	31
Defence Research Centre	
Library	32
Central Office	
Director General Army Development (NSO)	33–36
RAN Research Laboratory	
Library	37
Navy Office	
Naval Scientific Adviser	38
Directorate of Naval Aircraft Engineering	39
Army Office	
Army Scientific Adviser	40
Royal Military College	41
Air Force Office	
Aircraft Research and Development Unit, Scientific Flight Group	42
Air Force Scientific Adviser	43
Technical Division Library	44
Director-General—Aircraft Engineering	45
Department of Industry and Commerce	
Government Aircraft Factories	
Manager	46
Library	47

Department of Transport

Library		48
Flying Operations and Airworthiness Division		49

Statutory and State Authorities and Industry

Trans-Australia Airlines, Library		50
SEC of Victoria, Herman Research Laboratory, Library		51
Ansett Airlines of Australia, Library		52
Commonwealth Aircraft Corporation, Library		53
Rolls Royce of Australia Pty. Ltd., Mr. C. G. A. Bailey		54

Universities and Colleges

Adelaide	Barr Smith Library	55
Flinders	Library	56
La Trobe	Library	57
Melbourne	Engineering Library	58
Monash	Hargrave Library	59
Newcastle	Library	60
New England	Library	61
Sydney	Engineering Library	62
	Professor R. I. Tanner, Mechanical Engineering	63
	Professor B. W. Roberts, Mechanical Engineering	64
New South Wales	Physical Sciences Library	65
Queensland	Library	66
Tasmania	Engineering Library	67
Western Australia	Library	68
RMIT	Library	69

CANADA

NRC, Aeronautical and Mechanical Engineering Library 70

Universities

Memorial Uni. of Newfoundland, Professor D. V. Reddy 71

FRANCE

ONERA, Library 72

GERMANY

Fachinformationszentrum: Energie, Physik, Mathematik GMBH 73

INDIA

Defence Ministry, Aero Development Establishment, Library 74
Hindustan Aeronautics Ltd., Library 75
National Aeronautical Laboratory, Information Centre 76

JAPAN

National Aerospace Laboratory, Library 77

NETHERLANDS

National Aerospace Laboratory (NLR), Library 78

NEW ZEALAND

Transport Ministry, Airworthiness Branch, Library 79

SWEDEN

Aeronautical Research Institute, Library 80

SWITZERLAND

Armament Technology and Procurement Group 81
F+W (Swiss Federal Aircraft Factory) 82

UNITED KINGDOM		
CAARC, Secretary (NPL)		83
Royal Aircraft Establishment, Farnborough		84
National Physical Laboratory, Library		85
British Library, Lending Division		86
Aircraft Research Association, Library		87
Rolls-Royce Ltd., Aero Division, Bristol, Library		88
British Aerospace		
Kingston-upon-Thames, Library		89
Hatfield-Chester Division, Library		90
British Hovercraft Corporation Ltd., Library		91
Westland Helicopters Ltd.		92
Universities and Colleges		
Bristol	Engineering Library	93
London	Professor G. J. Hancock, Aero Engineering	94
Cranfield Institute of Technology	Library	95
UNITED STATES OF AMERICA		
NASA Scientific and Technical Information Facility		96
The John Crerar Library		97
Allis Chalmers Corporation, Library		98
Kentex Research Library		99
Lockheed-California Company		100
Lockheed Missiles and Space Company		101
Lockheed Georgia		102
McDonnell Aircraft Company, Library		103
United Technologies Corporation, Library		104
Universities and Colleges		
Florida	Aero Engineering Department	105
Massachusetts Institute of Technology	MIT Libraries	106
Spares		107-117

EN

DAT
FILME

6 8

DTI